

## Surface chemical bonding of selenium-treated GaAs(111) *A*, (100), and (111) *B*

T. Scimeca, Y. Watanabe, R. Berrigan, and M. Oshima

*NTT Interdisciplinary Research Laboratories, 3-9-11 Midori-cho, Musashino-shi, Tokyo 180, Japan*

(Received 19 May 1992)

The passivation of GaAs(100) by Se prepared *in situ* has been studied in detail by synchrotron-radiation photoelectron spectroscopy. Deposition of Se on GaAs with the substrate held at room temperature yields As-Se bonding with little reduction of band bending. Few changes are observed both in band bending and chemical bonding as the sample is heated to 250°C. In contrast, deposition of Se on GaAs at a substrate temperature of around 580°C gives rise to Ga-Se bonding as Se exchanges with As not only with the surface layer but penetrates into bulk layers as well. Finally, while the interfacial chemistry is similar to a great extent for the (111) *A* and (111) *B* surfaces, the uptake of Se in GaAs is found to vary in the following order: (111) *A* > (100) > (111) *B*. These results suggest that the Se uptake is controlled by the stability of the terminated atom for the different surface orientations.

### I. INTRODUCTION

While GaAs appears to be an excellent candidate for a variety of electronic devices, commercial development of GaAs technology has been hampered by the existence of a high number of surface and interfacial states that pin the Fermi level near midgap. Passivation of the GaAs surface by S in the form of either  $S^{-2}(aq)$  or  $(NH_4)_2S_x$  has shown drastic photoluminescence-yield gains,<sup>1,2</sup> increases in the current gains of heterostructure bipolar transistors,<sup>3</sup> as well as a Schottky-barrier-height dependence on the metal work function, all indicating that the GaAs surface-state density is significantly reduced.<sup>4</sup> Capacitance-voltage studies also show that the interfacial density of states is reduced by two orders of magnitude from  $\sim 10^{13}$  to  $\sim 10^{11}$   $cm^{-2} eV^{-1}$  when the GaAs surface is treated with  $(NH_4)_2S_x$ .<sup>5</sup>

Insight into the mechanism of this type of surface passivation has been provided recently by surface-sensitive photoemission spectroscopy.<sup>6-9</sup> The picture gradually emerging is that S only weakly bonds to As when GaAs is treated with the sulfur solution, but forms more stable bonds with Ga when the S-passivated wafer is heated in vacuum in the vicinity of 200°C. It is only when Ga-S bonding takes place that band bending is reduced and the full effect of the sulfur treatment is realized. This result is consistent with the reduction in  $As_{Ga}$  antisite defects as well as saturation of surface dangling bands with S.

Recently, Se (another group-VI element) in a variety of forms has also shown promise as a passivation material for GaAs.<sup>10-12</sup> Recently, dramatic photoluminescence gains for Se-treated GaAs have been reported.<sup>10,11</sup> The advantage in using Se is that one has the option of passivating *in situ* in a molecular-beam-epitaxy (MBE) chamber, since the vapor pressure is relatively low compared to sulfur. While the effects of Se passivation are now being explored, very little work up to now has been focused on understanding the mechanism of GaAs passivation by Se and on how it differs from passivation with sulfur.

In this paper, we report on the surface chemical bonding of Se to GaAs and how this is related to the temperature of the GaAs substrate during Se deposition. By doing this, we can explain, to a large extent, the basic nature of passivation for treatment that occurs in vacuum (e.g., Se) or *ex situ* ( $Na_2S$ ,  $Na_2Se$ , etc.). In addition, the uptake of Se is found to depend on the crystal face with greater uptake observed for the (111) *A* surface, lower uptake for the (100) surface, and the least uptake for the (111) *B* surface. This is correlated with the surface-atom desorption temperature for the three surfaces.

### II. EXPERIMENT

The samples were *n*-type GaAs wafers (Si doped) with a carrier density of  $1 \times 10^{18}$   $cm^{-3}$ . The GaAs wafers were first rinsed in acetone and then purified water before dipping in a commercial alkaline based etchant for 5 min. Following this, the sample was rinsed in purified water and dried with  $N_2(g)$ . The etched GaAs wafers were then attached to a Mo sample holder with In solder and placed in a vacuum chamber connected to both an analysis and MBE chamber.

Following this, the sample was heated in an As overpressure for about 5 min at 600°C to desorb any remaining oxides. The temperature was then lowered to about 550°C, where a GaAs epitaxial layer with an  $As_4/Ga$  flux ratio of about 10 was grown and a fine streaky  $2 \times 4$  reflection-high-energy-electron-diffraction (RHEED) pattern was observed. The substrate temperature was then lowered and the structure changed from  $2 \times 4$  to  $2 \times 1$ . The sample was then directly transferred from the MBE chamber to the analysis chamber.<sup>13</sup> Transferring of the sample from the MBE chamber to the analysis chamber and vice versa was achieved without breaking vacuum by a sample transfer mechanism. The experimental measurements were performed at the Photon Factory on beam line BL-1A in Tsukuba. Synchrotron-radiation photoemission (SRPES) and x-ray photoemission (XPS) spectroscopy (Al  $K\alpha$ ) measurements were then performed on the samples. Following this, the clean As-rich

GaAs sample was then transferred back to the MBE chamber where Se deposition was performed either at room temperature (RT) or at elevated temperatures near 580 °C. The temperature of the substrate in all cases was measured directly by an optical pyrometer. In the Se deposition, the effusion-cell temperature was kept at 130 °C during room-temperature deposition and 150 °C during deposition where the GaAs substrate was kept at 580 °C. The Se flux was measured by an ion-gauge flux monitor and was  $3.6 \times 10^{-6}$  torr at 130 °C and  $2.2 \times 10^{-5}$  torr at 150 °C.

The synchrotron photon energy was adjusted to 90.0 eV using a grating-crystal monochromator<sup>14</sup> with a  $1200\text{-mm}^{-1}$  grating to obtain surface-sensitive information on the Se 3*d*, As 3*d*, and Ga 3*d* core levels. The incident photon-energy calibration was made by directly measuring the Fermi edge of Au. The advantage of synchrotron radiation over conventional XPS in the analysis of Se is that the Se 3*d* cross section increases by over a factor of 50 as the incident photon energy is changed from 1486.6 eV (Al *K*α) to 90 eV, and that the electron mean free path decreases from about 15 to 5 Å. In addition to providing greater overall sensitivity as well as greater surface sensitivity, the synchrotron radiation is a bright source providing a photon flux of about  $10^{10}$ – $10^{11}$  photons/sec with an incident-energy resolution of about 0.3 eV as determined by the observed broadening of the Au Fermi edge.

### III. RESULTS AND DISCUSSION

#### A. Se/GaAs(100)

The Ga 3*d*, As 3*d*, and Se 3*d* SRPES spectra for clean As-rich GaAs, Se-passivated GaAs at substrate temperatures held at both room temperature and elevated temperatures, as well as the Se-desorbed Ga-rich state are presented in Figs. 1–3, respectively. Curve fitting of the spectra were performed to aid in interpretation. The  $3d_{5/2,3/2}$  spin-orbit coupling constants for Se 3*d*, As 3*d*, and Ga 3*d* were taken as 0.83, 0.60, and 0.45 eV, respectively.

The analysis begins with the As-rich clean GaAs surface. In Fig. 1, one can observe that the Ga 3*d* spectra is fit nicely with only one peak, as expected, since the surface is As terminated and, hence, one would only expect a single Ga peak that corresponds to Ga-As. In contrast, one can observe that the As 3*d* peak in Fig. 2 is significantly broader than the Ga 3*d* peak and fits nicely with two peaks separated by 0.4 eV, where the higher binding-energy peak corresponds to surface As, since one would not expect as much charge transfer for surface As as one would for As bonded to Ga in the third and deeper layers of GaAs.

The next set of spectra correspond to the case where GaAs was exposed at RT to a Se beam heated to 130 °C for 5 sec. One can see that the Ga 3*d* spectrum does not change in shape, nor is there any shift that one might associate with charge transfer and/or any associated changes in band bending. In contrast, drastic changes are observed in the As 3*d* spectra. In particular, a high binding-energy (BE) peak of large intensity is observed.

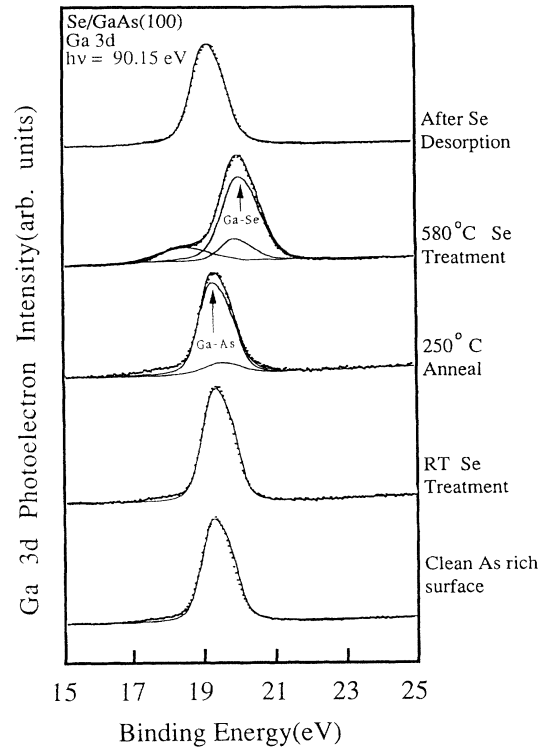


FIG. 1. The Ga 3*d* SRPES spectra plotted from bottom to top for the As-rich clean surface, the Se-deposited surface where the GaAs substrate was held at RT, the 250 °C-anneal case, the Se deposition where the GaAs substrate was heated at 580 °C, as well as after the Se was heated past the Se desorption temperature.

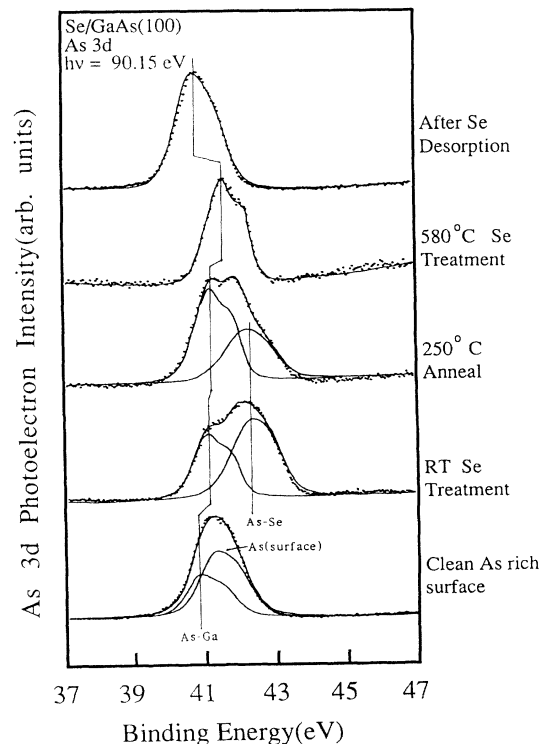


FIG. 2. The As 3*d* SRPES spectra plotted for the same sample preparation conditions listed in Fig. 1.

Based on the electronegativity values of Ga, As, and Se given as 1.82, 2.20, and 2.48, respectively,<sup>15</sup> one can assign the high BE peak as originating from an As-Se peak with a slight formal positive charge localized on the As atom, since Se is the more electronegative element. Further, the As peak corresponding to Ga-As is shifted very little from the Ga-As peak for the clean surface. This is in agreement with the small binding-energy shift for the Ga 3*d* spectrum shown in Fig. 1. Furthermore, there is very little change in the Ga 3*d* spectra between the clean GaAs surface and the Se-treated GaAs surface, indicating that there is no interaction between Ga and Se at this stage. The corresponding Se 3*d* spectrum is shown in Fig. 3. The wide full width at half maximum (FWHM) of the Se 3*d* peak is attributed in part to the relatively large 0.83-eV 3*d*<sub>3/2,5/2</sub> spin-orbit coupling constant of Se 3*d*. The spin-orbit splitting value for Se was estimated from the amorphous Se 3*d* spectra under high resolution since only one state exists. The spectrum is composed of two peaks with the low BE being ascribed to Se-As and the large BE peak ascribed to Se that overlays the Se bonded to As. Separate measurements on thick amorphous Se layers yield a binding energy of 55.1 eV, indicating that the high BE peak is not due to amorphous Se, but due to Se bound to As at the GaAs surface.

In Fig. 4, the valence-band edge measurements indicate that band bending is on the order of 0.8 eV for both the clean As-rich surface as well as Se-deposited GaAs surface, indicating that the surface states on the GaAs surface are not significantly reduced when the Se deposition is performed at RT.

The next step involved heating the GaAs substrate to 250 °C for 10 min in vacuum. In the case of GaAs treated with (NH<sub>4</sub>)<sub>2</sub>S<sub>x</sub>, S was observed to replace As, bond with Ga, and reduce band bending at an annealing tempera-

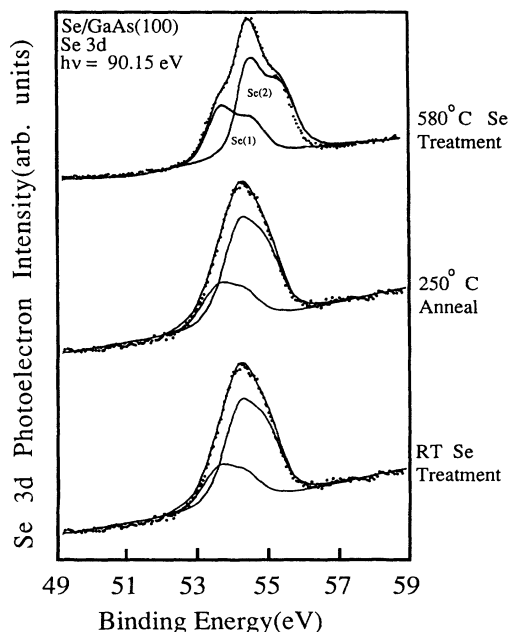


FIG. 3. The Se 3*d* SRPES spectra plotted for the same sample preparation conditions listed in Fig. 1.

ture of approximately 200 °C.<sup>8,9</sup> The Ga 3*d* spectrum for the Se-treated GaAs surface annealed at 250 °C is shown in Fig. 1. In this case, there is a slight spectral broadening that is indicative of Ga bonding not only to As, but to Se as well. The Ga-As peak-position determination was aided by deconvoluted As 3*d* and valence-band edge measurements, as shown in Figs. 2 and 4, respectively. In this case, very little band-bending reduction was observed. The results of Fig. 1 demonstrate that there is very little As-Se exchange and, hence, very little Ga-Se bonding even with the 250 °C anneal. Nevertheless, the curve fitting is somewhat difficult for the Ga 3*d* spectrum, since the Ga-As and Ga-Se binding-energy shifts are small, owing to the similar electronegativity values of As and Se.

Larger spectral changes are observed for the As 3*d* spectrum, as shown in Fig. 2. In this case, the Ga-As peak grows in relative intensity and the As-Se peak decreases by about half of its original intensity, indicating that about half of the surface As is desorbed by annealing. The interpretation of the Se 3*d* spectra for the 250 °C anneal is quite complex, owing to the mixture of four states: As-Se(1), As-Se(2), Ga-Se(1), and Ga-Se(2). In addition, very little spectral change was observed for the Se 3*d* spectra between the clean surface and the 250 °C surface. From the valence-band results, very little band flattening is observed for this annealing, suggesting

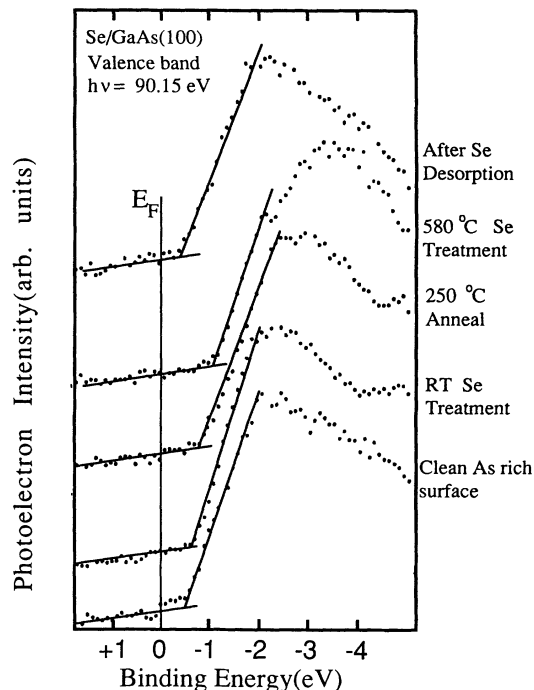


FIG. 4. The valence-band spectra plotted with the sample conditions shown on the right-hand side of the figure. In this case, the Fermi level  $E_F$  was determined by the Au Fermi level. Band-bending values can be obtained by subtracting the valence-band edge from the band gap for GaAs (1.43 eV). Thus, a reduction of band bending corresponds to an increase in binding energy for the valence-band edge.

that the GaAs surface is not passivated at this point, since there are still a large number of surface-defect states giving rise to the relatively high band bending. These results also suggest that the chemistry of Se and S passivation are quite different. As mentioned above conversion of As-S to Ga-S takes place with nearly 100% conversion at temperatures well below 250°C, suggesting the activation-energy barrier for this conversion is considerably lower than the As-Se to Ga-Se conversion. This is nonetheless not very surprising based on the greater ionicity and greater heat of formation of Ga-S relative to Ga-Se.<sup>16</sup>

The next step involved an additional GaAs sample and preparing the sample in the MBE chamber in a manner similar to that described before. The Ga 3*d*, As 3*d*, and valence-band spectra were virtually identical for the As-rich clean GaAs surfaces for the two different samples, ensuring that the surfaces and starting conditions were also virtually identical. Following this, the sample was heated in an As<sub>4</sub> overpressure at 550°C. During this time, the GaAs wafer was then exposed to a Se beam operating at 150°C. During this time, the As-beam shutter was shut and the sample was exposed to the Se flux for 5 min. Following this, the sample was cooled and continuously exposed to a Se flux until the sample temperature reached 400°C, at which time the Se shutter was closed and the sample was transferred to the analysis chamber. A 2×1 RHEED pattern was observed prior to Se treatment and was maintained with Se treatment.

The results of the high-temperature Se passivation are shown in Figs. 1–4. The Ga 3*d* spectra peak shows a significant shift to higher binding energy on the order of 0.4 eV. This high binding-energy shift is attributed to a reduction in band bending, as one can see directly in the higher BE shift of the valence-band edge. The Ga 3*d* peak has two main components attributed to a bulk Ga-As and Ga-Se peak and explains the broader FWHM. In contrast, the As 3*d* peak is rather simple and is fit with only one peak, clearly indicating that any last vestiges of As-Se bonding have disappeared. In addition, the As 3*d* spectrum as a whole shifts to higher binding energy, especially with respect to the As-Ga component of the previous 250°C-anneal As 3*d* spectra. The Se 3*d* spectrum for the 580 °C Se deposition is shown in Fig. 3. In this case, the spectral shape becomes better defined, but there is no question that there are two different Se atoms. The large spin-orbit splitting of 0.83 eV gives the final spectra a shape where three large peaks are observed. The 3*d*<sub>5/2</sub> component of the lower-BE Se peak nearly coincides with the 3*d*<sub>3/2</sub> component of the higher-BE Se peak. The higher-BE Se is assigned to surface Se. The lower-BE Se is attributed to Se in the third and possibly fifth layers of GaAs substituting with As. In this case, one would expect a lower BE for Se incorporated below the GaAs surface layer, since one would expect more complete charge transfer from Ga to Se, since Se is coordinated to four Ga atoms. In contrast, surface Se for the (100) case is only coordinated to two Ga atoms, hence, one would expect a higher binding energy since there is less charge transfer from Ga to Se.

The picture that emerges can be visualized more easily

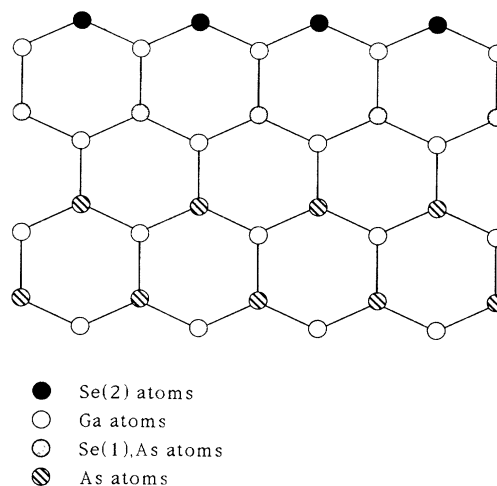


FIG. 5. A side projection of the Se-passivated GaAs(100) surface that would correspond to Se passivation when the GaAs substrate is held at elevated temperatures. On the basis of the relative intensities of the two Se 3*d* peaks observed in Fig. 3, the third and possibly fifth layers are not completely occupied by Se. See the text for a more detailed discussion. Nevertheless, one can see that the dangling bonds from surface As atoms are eliminated to a great extent when Se exchanges with As atoms at the top surface layer.

in Fig. 5, which is a side view of the Se-passivated GaAs(100) surface. The first surface layer is terminated with Se atoms with no dangling bonds, since Se is a group-VI atom. The third layer has a fraction *x* of Se atoms substituting for As atoms and a fraction (1−*x*) of As atoms that remain. One may expect this fraction to depend on conditions such as substrate temperature, Se pressure, etc. Based on the relative peak areas of the surface and bulk Se 3*d* peaks, a value of 0.90 was obtained for the Se incorporation in the third layer. This assumes there is no As-Se exchange in the deeper layers, most notably the fifth layer as reported by Chambers and Sundaram<sup>17,18</sup> in their recent angle-resolved XPS work. However, as discussed later, the uptake of Se depends on the crystal face and substrate temperature with As-Se exchange in the fifth layer occurring at high substrate temperatures.

One may contrast *in situ* passivation with *ex situ* passivation by either S or Se. If the passivation is not done in vacuum at elevated temperatures above 400°C, one would not expect the passivating atoms (S or Se) to penetrate below the surface layer. This is because the bulk-As atoms are not desorbed in vacuum until one reaches this temperature. In *ex situ* passivation, all but a monolayer of S or Se is believed to adhere to the GaAs surface after the treated surface is placed in vacuum. Even after heating above 480°C,<sup>8</sup> no movement of S to bulk has been observed. Thus, *ex situ* passivation of GaAs by treatment outside vacuum can only passivate the surface layer. The key point is that if defect states also exist near the surface, such as As<sub>Ga</sub> antisite atoms, then a passivation scheme where insertion of Se into buried defects near the surface may be advantageous over passivation techniques where insertion is not possible.

TABLE I. A summary of the band-bending measurement results for both S and Se passivation.

Sulfur passivation	Band bend (eV)	Selenium passivation	Band bend (eV)
Clean surface (As rich)	0.8	Clean surface (As rich)	0.9
As-S	0.8	As-Se (RT)	0.75
Ga-S	0.5	250 °C anneal	0.75
		Ga-Se (550 °C)	0.3
After S desorption	1.0	After Se desorption	1.0

The band-bending results suggest that while the band bending is not quite eliminated with Se passivation, there is an improvement of Se passivation over S passivation by 0.1–0.2 eV. The relative differences in band bending for *ex situ* S passivation and *in situ* Se passivation are also presented in Table I.

Finally, the sample was heated in the analysis chamber in vacuum until the Se was desorbed, which, for the GaAs(100) crystal face, was at about 630 °C. The Ga-rich (100) spectra show a large number of defect states and a spotty RHEED pattern, as well as increased band bending.

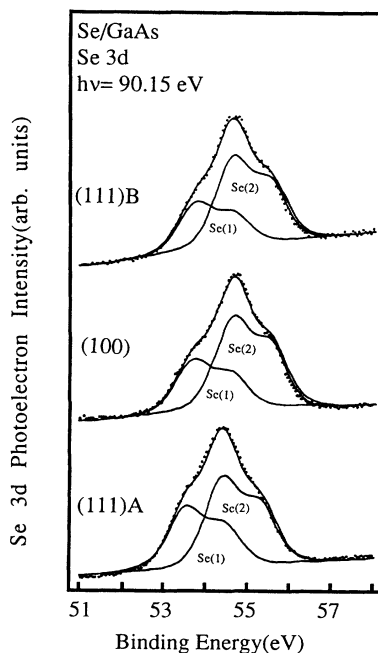


FIG. 6. The Se 3d photoelectron spectra for Se/GaAs(111)A, (100), and (111)B surfaces are plotted. For all three systems, the substrate temperature was held at 580 °C and exposed to a Se flux for 5 min. The differences are attributed to differences in Se uptake between the three different orientations where Se(1) corresponds to Se incorporated into GaAs and Se(2) corresponds to surface Se.

### B. Chemical bonding differences among the Se/GaAs(111)A, (100), and (111)B surfaces

In addition to the Se/GaAs(100) surface, measurements were also performed on the Se/GaAs(111)A and (111)B surfaces. One may expect some differences, since the coordination number of the surface-terminated atom to Ga is 1, 2, and 3 for the (111)A, (100), and (111)B surfaces, respectively. The Se 3d spectra for the three different surfaces are shown in Fig. 6. After peak fitting, one can observe that the Se(1)/Se(2) or surface Se/bulk Se ratio is greatest for the (111)A surface and lowest for the (111)B surface. Assuming an electron mean free path of 6 Å, calculations on the relative Se(1) and Se(2) intensities indicate Se third-layer occupation of 0.86, 0.90, and 1.0 for the (111)B, 100, and (111)A surfaces, respectively. In addition, a Se occupancy of 0.18 is obtained for the fifth layer for the (111)A surface. What this indicates is that the uptake of Se in bulk GaAs is greatest for the (111)A surface. This result is reasonable, since the desorption temperature for the surface-terminated atom is lowest for the (111)A surface and greatest for the (111)B surface. While the surface As desorption temperature was not measured in this experiment for the three surfaces, the Se desorption temperatures were measured by *in situ* SRPES for the three surfaces under equivalent heating rates of 10 °C/min. These results are consistent with the S/GaAs

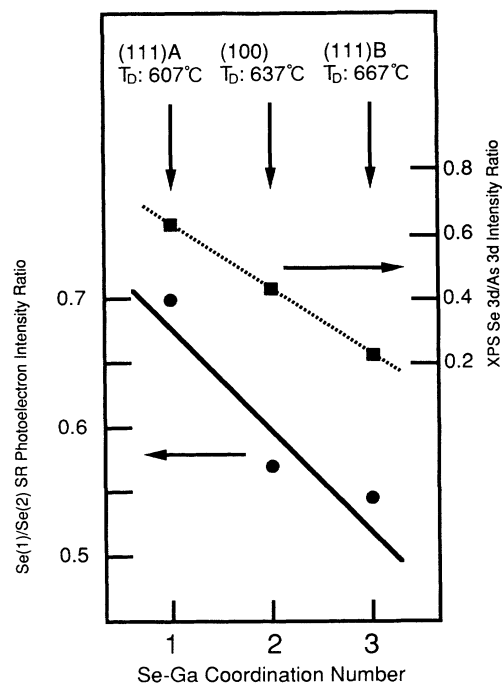


FIG. 7. The Se(1)/Se(2) or surface Se/bulk Se SR photoelectron intensity is plotted (left vertical axis) against the Se-Ga coordination number. In addition, the Se uptake is also reflected in the Se 3d/As 3d XPS intensity ratio where a greater uptake is observed for the (111)A surface which has the lowest Se desorption temperature ( $T_d$ ). In contrast, the (111)B surface has the highest Se desorption temperature, since surface Se is bonded to three Ga atoms and thus the degree of Se-As exchange is relatively small.

desorption work reported previously and is fully consistent with the surface-atom-Ga-binding-energy strength. Thus, the uptake of Se in bulk GaAs at substrate temperatures near the surface-As desorption temperature is controlled by the desorption of bulk As, which causes bulk As to diffuse to the surface where it is also desorbed. Ultimately, the As vacancies are filled by Se atoms during Se exposure and hence the degree of Se uptake is observed to depend on crystal orientation, which is, in turn, related to the surface-As desorption temperature. To confirm this, the Se 3d/As 3d XPS intensity ratio was also measured and is plotted on the right vertical axis in Fig. 7. In this figure, the left vertical axis corresponds to the Se(1)/Se(2) or surface Se/bulk Se SR photoelectron intensity ratio and is plotted for the three different surfaces as a function of the Se-Ga coordination number. The Se desorption-temperature values are also shown in the top of the figure. While the greater uptake of Se is observed for the (111)A surface, no significant changes in band ending or other spectral features (e.g., As 3d, Ga 3d, etc.) were observed, indicating that band-bending reduction is achieved at relatively low coverages. This topic will be addressed in another paper shortly.

#### IV. CONCLUSION

The passivation of GaAs by Se in vacuum has been clarified by surface-sensitive SRPES. The results indicate

that passivation of GaAs does not occur when the substrate is held at RT during Se deposition. Furthermore, the activation barrier for As-Se to Ga-Se is a bit higher than the As-S to Ga-S barrier. It is found that even at 250 °C, surface As still remains even if it is bonded to Se and that band bending is not significantly reduced. In contrast, if deposition is made at a relatively high temperature, surface As is completely substituted by Se and, in addition, there is a certain amount of As-to-Se substitution in the third and fifth buried layers. With Se bonding exclusively to Ga and the disappearance of surface As, band bending is reduced (but not eliminated) considerably to a value of about 0.4 eV.

Furthermore, the uptake of Se in bulk GaAs was found to depend on the surface crystal orientation with greatest Se uptake for the (111)A surface, lower uptake for the (100) surface, and even lower uptake for the (111)B surface. These results are explained by the relative stability of surface As for the three surfaces.

#### ACKNOWLEDGMENTS

We would like to thank H. Ando for the monochromator adjustment and H. Maeda for developing a peak deconvolution program used in the data analysis. We also gratefully acknowledge the encouragement and support of Dr. Y. Ishii.

- 
- <sup>1</sup>C. J. Sandroff, M. S. Hegde, L. A. Farrow, R. Bhat, J. P. Harbison, and C. C. Chang, *J. Appl. Phys.* **67**, 586 (1990).  
<sup>2</sup>J. Fan, Y. Kurata, and Y. Nannichi, *Jpn. J. Appl. Phys.* **28**, L2255 (1988).  
<sup>3</sup>C. J. Sandroff, R. N. Nottenburg, J.-C. Bischoff, and R. Bhat, *Appl. Phys. Lett.* **51**, 33 (1987).  
<sup>4</sup>J. Fan, H. Oigawa, and Y. Nannichi, *Jpn. J. Appl. Phys.* **27**, L2125 (1988).  
<sup>5</sup>M. S. Carpenter, M. R. Melloch, and T. E. Dungan, *Appl. Phys. Lett.* **53**, 66 (1988).  
<sup>6</sup>C. J. Spindt, D. Liu, K. Miyano, P. L. Meissner, T. T. Chiang, T. Kendelewicz, I. Lindau, and W. E. Spicer, *Appl. Phys. Lett.* **55**, 861 (1989).  
<sup>7</sup>K. M. Geib, J. Shin, and C. W. Wilmsen, *J. Vac. Sci. Technol.* **B 8**, 838 (1990).  
<sup>8</sup>H. Sugahara, M. Oshima, R. Klauser, H. Oigawa, and Y. Nannichi, *Surf. Sci.* **242**, 335 (1991).  
<sup>9</sup>T. Scimeca, Y. Muramatsu, M. Oshima, H. Oigawa, and Y. Nannichi, *Phys. Rev. B* **44**, 12 927 (1991).  
<sup>10</sup>C. J. Sandroff, M. S. Hegde, L. A. Farrow, R. Bhat, J. P. Harbison, and C. C. Chang, *J. Appl. Phys.* **67**, 586 (1990).  
<sup>11</sup>F. S. Turco, C. J. Sandroff, M. S. Hedge, and M. C. Tamargo, *J. Vac. Sci. Technol.* **B 8**, 856 (1990).  
<sup>12</sup>S. Takatani and M. Nakazawa, in *Modification of GaAs(100) Surface by Se and Formation of Amorphous-Se/GaAs(100) Heterostructure*, Proceedings of the International Symposium on GaAs and Related Compounds, edited by K. E. Singer, IOP Conf. Proc. No. 112 (Institute of Physics, Bristol, 1990), Chap. 3, p. 111.  
<sup>13</sup>M. Oshima, T. Kawamura, S. Maeyama, and T. Miyahara, *J. Vac. Sci. Technol. A* **6**, 1451 (1988).  
<sup>14</sup>T. Kawamura, S. Maeyama, M. Oshima, Y. Ishii, and T. Miyahara, *Rev. Sci. Instrum.* **60**, 1928 (1989).  
<sup>15</sup>L. Pauling, *The Nature of the Chemical Bond*, 3rd ed. (Cornell University Press, Ithaca, 1960).  
<sup>16</sup>O. Kubaschewski and C. B. Alcock, *Metallurgical Thermochemistry*, 5th ed. (Pergamon, New York, 1979).  
<sup>17</sup>S. A. Chambers and V. S. Sundaram, *Appl. Phys. Lett.* **57**, 2342 (1990).  
<sup>18</sup>S. A. Chambers and V. S. Sundaram, *J. Vac. Sci. Technol. B* **9**, 2256 (1991).  
<sup>19</sup>T. Ohno and K. Shiraishi, *Phys. Rev. B* **42**, 11 194 (1990).  
<sup>20</sup>T. Ohno (private communication).

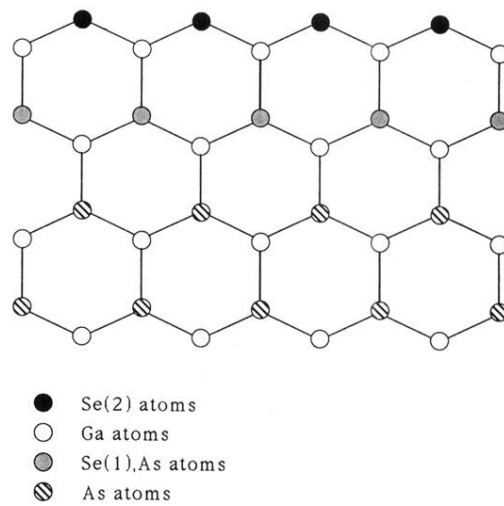


FIG. 5. A side projection of the Se-passivated GaAs(100) surface that would correspond to Se passivation when the GaAs substrate is held at elevated temperatures. On the basis of the relative intensities of the two Se  $3d$  peaks observed in Fig. 3, the third and possibly fifth layers are not completely occupied by Se. See the text for a more detailed discussion. Nevertheless, one can see that the dangling bonds from surface As atoms are eliminated to a great extent when Se exchanges with As atoms at the top surface layer.